Corrosion Behaviour and Cell Viability of Untreated and Laser Treated Ti6Al7Nb Alloys

MIHAELA MINDROIU[1], CRISTIAN PIRVU[1,*], BIANCA GALATEANU[2], IOANA DEMETRESCU[1]

[1] University Polytechnic of Bucharest, Faculty of Applied Chemistry and Materials Science, 1-7 Polizu, 011061, Bucharest, Romania

[2] University of Bucharest, Research Center for Biochemistry and Molecular Biology, 91-95 Independentei, 76201, Bucharest, Romania

The paper's aim is to evaluate the corrosion behaviour for the TiO_2 oxide film native and obtained using laser texturing procedure. The chosen working conditions lead to grooves on treated sample which can be used to increase the bone implants strength. A better cell viability was observed after 24 h, but for longer period of time (48 h) was decreased.

Keywords: Ti6Al7Nb alloy, scanning electronic microscopy, atomic force microscopy, contact angle, electrochemical impedance spectroscopy.

Despite the fact that titanium is a very good implant metallic biomaterial due to its excellent properties regarding low density, stability in bioliquids and biocompatibility, alloying is frequently performed [1]. Titanium alloys are actually preferred in bioapplications in orthopedics and dental surgery, because of the necessity to enhance mechanical properties [2]. The alloy with vanadium was extensively exploited as an implant biomaterial, but appears to be toxic [3]. Thus, Ti6Al7Nb is increasingly interesting for bioapplications, and various procedures of activation and bioactivation have been developed in the last decade in order to enhance its stability and biocompatibility. As Ti and other Ti alloys, Ti6Al7Nb readily passivates to form a protective oxide layer [4], containing predominantly TiO_2 oxide, which exhibits especially ionic conductivity at the redox potential in biosystems. The protection capacity of the oxide strongly depends on the growth procedure. A large variety of techniques of surface modifications [5-8] have been elaborated on Ti and Ti alloys, such as: plasma spraying [9], anodizing [10-12], laser deposition [13-16], thermal treatment [17, 18].

The present paper aims to investigate the behaviour of laser-textured Ti6Al7Nb bioalloy, to compare the electrochemical behaviour and the biocompatibility of titanium oxide surfaces obtained by laser treatment with those of a TiO_2 thin film naturally grown. This approach is related to the idea that all surface modification aspects are important in cell growth but their behaviour is not entirely predictable [19, 20]. The TiO_2 modified surfaces were characterized by surface analysis and the electrochemical behaviour was also investigated after immersion in Fusayama artificial saliva.

A series of studies show that phenomena occurring during laser texturing treatment cause melting and then fast crystallization, that is accompanied by internal stresses and appearance of cracks or/and grooves on the surface, which can significantly influence the interface behaviour in biofluid [21-23]. The size of cracks/grooves and pores, shape, volume fraction, and distribution, which have a major influence on mechanical and biological properties and corrosion behaviour, are generally difficult to control [24]. According to literature data, however, the existence of grooves may be used for the enhancement of bone-implant strength [25].

The working conditions chosen for this study lead to the appearance of grooves and cracks during laser treatment on Ti6Al7Nb. Consequently, the study is directed to surface features influences on electrochemical behaviour, ion release and material biocompatibility.

Experimental part

Materials and Instrumentation

The substrate was Ti6Al7Nb alloy; it was prepared by the Institute for Non-ferrous and Rare Metals (Bucharest, Romania) with the composition indicated previous by Al 5.88 %, Nb 6.65 %, Fe 0.3 %, H 0.012 %, N 0.05 %, O 0.2 %, C 0.1 %, Titan rest [26].

The biomaterials samples had 2 mm thickness and 1 cm diameter in exposure. The surface pre-treatment consisted in: abrasion, chemically polishing in 20 % HNO_3 + 3 % HF for 10 min , degreasing for 5 min in boiling benzene and rinsing thoroughly with distilled water. Laser texturing was obtained using an ablation laser system Nd: YAG at 266 nm wavelength. On Ti6Al7Nb alloy, the surface supposed to be textured was delimitated via concentric spots with 155 μm diameters on a total surface of 16 mm^2. Working laser parameters were set as follows: scanning surface rate 5 $\mu m.s^{-1}$ and laser energy 2 $J.pulse^{-1}$. The angle of incidence of the beam with respect to the sample surface was 90°. The delimitated surface was scanned with a typical repetition rate of 10 Hz. All surface irradiations were performed under ambient conditions.

Samples surface characterization

The surface characterization was achieved by means of the following techniques: Scanning Electronic Microscopy (SEM) using FEI/Phillips XL30 ESEM with EDAX (X-rays emission) to infer the distribution of chemical constituents, Atomic Force microscope (AFM) from APE Research (in contact mode) to deduce the roughness, and Optical Microscope Carl Zeiss Axio Scope A1 to infer the phase identification. The contact angle measurements were performed in order to evaluate the wettability of the modified surface as a result of changing structure and

* *email: c_pirvu@chim.pub.ro; Tel.: 040214023930*

composition. They were carried out with 100 Optical Contact Angle Meter - CAM 100.

Electrochemical behaviour of the samples

Electrochemical stability was evaluated from the open circuit potential, Tafel plots and electrochemical impedance spectroscopy (EIS). Measurements in open circuit were performed with an electronic voltammeter type MATRIX 20, and all the other electrochemical stability measurements were conducted using an Autolab PGSTAT 302 N with GPES and NOVA specific software.

The electrochemical systems consisted in three electrodes immersed in a single-compartment cell, and using platinum as a counter-electrode, Ag/AgCl as reference electrode and Ti6Al7Nb alloy as working electrode. To substantiate the anticorrosion properties, the Tafel regions of cathodic and anodic polarization curves were extrapolated. Tafel plots were obtained by polarization with ± 150 mV *vs.* Ag/AgCl toward electrode potential in anodic direction with a scan rate of 2 $mV.s^{-1}$. The EIS measurements were conducted at free potential in each studied solution and in the frequency domain between 0.01 and 10.000 Hz with amplitude of ±10 mV *vs.* Ag/AgCl. EIS analyses were discussed in term of Nyquist representations. The dissolution rate was obtained by determinations of ions release using ICP-Mass Spectrometry method (Perkin Elmer SCIEX). The tested electrochemical bioliquid was Fusayama artificial saliva with an important calcium content as following: NaCl 0.400 $g.L^{-1}$, KCl 0.900 $g.L^{-1}$, $CaCl_2 \cdot 2H_2O$ 0.795 $g.L^{-1}$, NaH_2PO_4 0.690 $g.L^{-1}$, Urea 1.000 $g.L^{-1}$.

Biological assays. Cell culture and cell viability

Human osteoblast cells (line G292, American Type Culture Collection) were seeded at an initial density of $1 . 10^4$ $cells.cm^{-2}$ in a Dulbecco's Modified Eagle Medium (DMEM) containing 10 % fetal bovine serum (FBS) and 100 $U.mL^{-1}$ penicillin and 100 $\mu g.mL^{-1}$ streptomycin, in a humidified atmosphere of 5 % CO_2. Cells were plated at the same density on untreated and treated discs; the evolution of cell culture was monitored using an inverted phase contrast microscope NIKON Elipse TS 100 to asses the cell morphology. To estimate the density of viable cells by measuring mitochondrial dehydrogenase activity (3-(4, 5-dimethylthiazolyl-2)-2, 5-diphenyltetrazolium bromide) was employed as MTT assay [27, 28]. MTT assay measures the cell activity, proliferation rate and cell viability. The yellow tetrazolium MTT was reduced by metabolically active cells to the corresponding blue formazan in part by the action of dehydrogenases. The absorbance (DO) measured at a wavelength of 570 nm is proportional with the number of viable cells. The determinations were performed at 2 different times, at 24 and 48 h from the initial seeding. An ImageJ program was used for the statistical treatment of biocompatibility data.

Results and discussions

Surface analysis

The SEM images of Ti6Al7Nb surface after laser treatment is presented in figure 1.

Morphological structures of untreated Ti6Al7Nb alloy have already been presented in literature [29], indicating the presence of β phase enriched in Nb, and an μ phase enriched in Al grains.

After the surface melting during laser treatment, the microstructure transforms to larger grains embedded in the prior β matrix; this behaviour was also described in literature for Ti6Al4V alloy [12]. The higher oxygen content

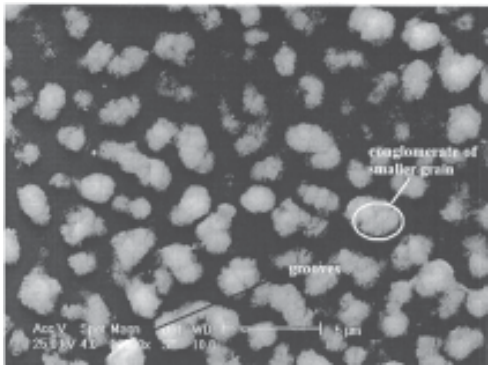

Fig. 1. SEM morphological image of Ti6Al7Nb surface after laser treatment

and the variation of Ti, Al and Nb content were observed, indicating the formation of more oxides after ablation, despite the fact that laser-treated surface is thicker. According to literature data [30] the oxide phases of Ti, Al and Nb were detected on Ti6Al7Nb alloy by XRD.

From the ratio oxygen to Ti, Al, and Nb, Al appears to be less involved in the oxide formation, as seen in table 1. The EDAX module of SEM enabled the computation of the amount of oxygen in the film obtained via laser treatment. This was 16.63 wt %, with 10 wt % higher than the untreated alloy, where the amount was 6.67 wt %.

Table 1
ELEMENTAL COMPOSITION FROM EDAX SPECTRA

Element	wt % Natural passivated surface	wt % Textured surface
O	6.67	16.63
Al	5.92	5.18
Nb	7.56	5.45
Ti	79.85	72.74
Total	100	100

The SEM image of textured Ti6Al7Nb surface (fig. 1) indicates the formation of an oxide layer covering the entire surface and having a granular structure with diameters from 1 μm to 3 μm. Between big grains, with diameters of around 3 μm, different vacancies can be observed that appear as grooves and cracks. The bigger grains are conglomerates of smaller grains, with a diameter of around 0.6 μm.

The topographical features of oxides are evaluated from AFM images as well. Figure 2 shows two and three-dimensional images for untreated and modified by laser treatment Ti6Al7Nb.

According to figure 2, AFM surface analysis of untreated and treated Ti6Al7Nb alloy indicate the formation of a granular oxide layer as droplets and cluster/aggregates of micron size, as showed by SEM. The film covered the entire surface, and the visible cracks and grooves appear at the grains boundary.

The values of average roughness (R_a) which correspond to untreated and treated Ti6Al7Nb alloys are 38 nm and 89 nm respectively.

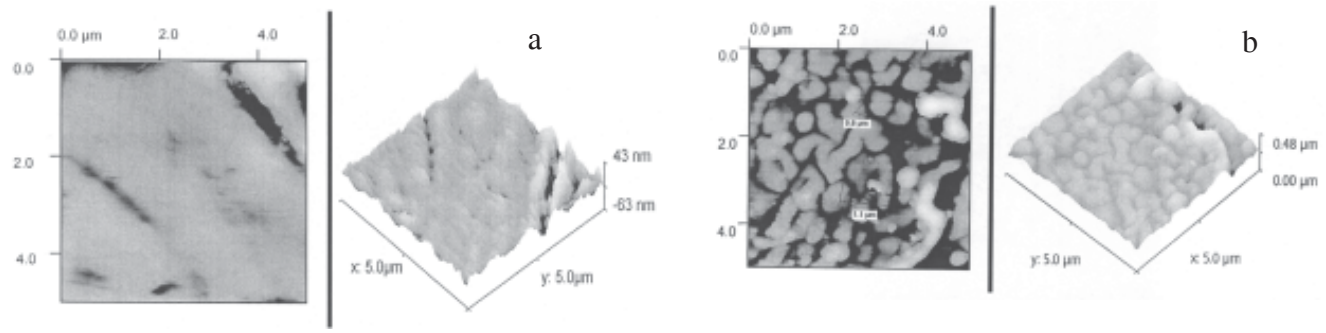

Fig. 2. Two and three-dimensional images for untreated (a) and modified by laser treatment (b) Ti6Al6Nb

The laser treated surface has slightly higher roughness values, which may have positive influence on subsequent interaction with biological environment, being known the correlation between surface roughness and bio-compatibility.

Contact angle is also one of numerous physical features of the surface that affects the cell response. The contact angle value corresponding to untreated Ti6Al7Nb is about 85.89°, while for laser treated alloy it is 79.35°, indicating a slight improvement of hydrophilic character for the oxide surface growth by laser treatment compared to untreated surface.

Electrochemical behaviour

The variation of the open circuit potential (OCP) for untreated and treated Ti6Al7Nb samples for 65 days immersion in Fusayama saliva is presented in figure 3.

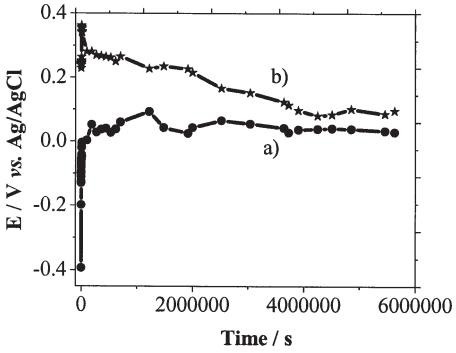

Fig. 3. Evolution of the open circuit potential for 65 days immersion in Fusayama saliva in the case of (a) untreated and (b) laser treated Ti6Al7Nb

The OCP evolution indicates the thermodynamic tendency of titanium alloy to oxidation. Untreated Ti6Al7Nb alloy has a value of -390 mV *vs.* Ag/AgCl at the initial immersion time, while laser treated Ti6Al7Nb surface has a value of more than 600 mV.

After a short immersion time, *OCP* for untreated alloy is shifted to positive potentials reaching then to a pseudo steady-state. The variation with time of *OCP* is due to the changes that occur in the nature of the electrode surface (oxidation, formation of the passive layer) improving its corrosion protection ability by decreasing the metal dissolution.

Afterwards, the *OCP* increases slowly during 300 h reaching a pseudo steady-state of about 50 mV *vs.* Ag/AgCl, which suggests the surface modification due to the growth of the compact oxide film onto the metallic surface.

For the treated sample, the potential has fluctuations in the range of 250÷320 mV *vs.* Ag/AgCl in the first 24 h, followed by a slow decrease to about 100 mV *vs.* Ag/AgCl and eventually a steady-state after 40 days.

This behaviour supports the presence of a surface which has species in various oxides states, some of them being less stable and able to generate porosity and/or cracks via dissolution, which can promote the electrolyte penetration. These phenomena occur especially after 24 h, when the potential begins to decrease to more negative values due to the changes on the surface. Repassivation is taking place in time and the protective film appears.

Tafel diagrams for Ti6Al7Nb/oxide electrodes obtained after laser treatment and immersion in Fusayama saliva for short time (1 h) and for 1, 2, 7, and 14 days are presented in figure 4b. The experimental polarization results were obtained by scanning in anodic direction with a scan rate of 2 mV.s^{-1}.

Table 2 is devoted to electrochemical parameters from Tafel plots. It should be pointed out that the observed corrosion potentials are higher for treated sample comparing with untreated sample for the same immersion time. After 14 days of immersion in Fusayama saliva the Tafel plots indicate changes which induce a difference of about 300 mV *vs.* Ag/AgCl between treated and untreated samples.

On the other hand, the presence of more positive values of the corrosion potential and the higher values of corrosion current (i_{corr}) for treated samples can be attributed to the cracks and grooves in the surface oxide microstructure at the grain boundary for laser treated samples.

The corrosion current on untreated samples decreases by an order of magnitude in the first 24 h of immersion suggesting a rapid passivation of the surface as was observed in the OCP measurements.

On contrary, for the treated sample the corrosion current remains almost constant during the first 24 h, due to the stability of the oxide layer obtained by laser treatment, then it increases after 48 h due to electrolyte penetration and finally decreases due to repassivation of the surface.

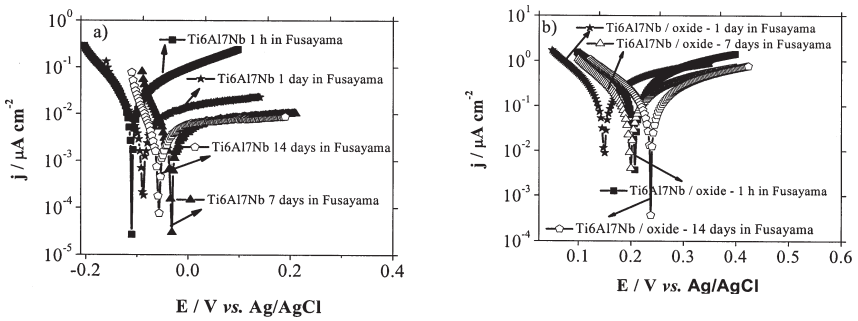

Fig. 4. Tafel plots for untreated Ti6Al7Nb (a) and laser treated Ti6Al7Nb (b) immersed in Fusayama saliva

Sample / immersion time	i_{corr}, ($A.m^{-2}$)	E_{corr}, (mV)	R_p, ($\Omega.m^2$)	V_{corr}, ($mm.year^{-1}$)
Untreated Ti6Al7Nb / 1 h	$1.143 \cdot 10^{-3}$	-117	$0.973 \cdot 10^{+2}$	$1.035 \cdot 10^{-3}$
Untreated Ti6Al7Nb / 1 day	$2.672 \cdot 10^{-4}$	-72	$4.577 \cdot 10^{+2}$	$2.326 \cdot 10^{-4}$
Untreated Ti6Al7Nb / 2 days	$1.646 \cdot 10^{-4}$	-65	$4.668 \cdot 10^{+2}$	$1.433 \cdot 10^{-4}$
Untreated Ti6Al7Nb / 7 days	$1.504 \cdot 10^{-4}$	-32	$4.804 \cdot 10^{+2}$	$1.310 \cdot 10^{-4}$
Untreated Ti6Al7Nb / 14 days	$1.031 \cdot 10^{-4}$	-57	$5.170 \cdot 10^{+2}$	$8.970 \cdot 10^{-5}$
Treated Ti6Al7Nb / 1 h	$1.820 \cdot 10^{-2}$	207	$0.555 \cdot 10^{+1}$	$1.584 \cdot 10^{-2}$
Treated Ti6Al7Nb / 1 day	$1.892 \cdot 10^{-2}$	149	$0.437 \cdot 10^{+1}$	$1.647 \cdot 10^{-2}$
Treated Ti6Al7Nb / 2 days	$3.471 \cdot 10^{-2}$	160	$0.425 \cdot 10^{+1}$	$3.022 \cdot 10^{-2}$
Treated Ti6Al7Nb / 7 days	$1.009 \cdot 10^{-2}$	199	$1.86 \cdot 10^{+1}$	$1.001 \cdot 10^{-2}$
Treated Ti6Al7Nb / 14 days	$9.635 \cdot 10^{-3}$	238	$1.901 \cdot 10^{+1}$	$8.718 \cdot 10^{-3}$

Table 2
ELECTROCHEMICAL PARAMETERS FROM TAFEL PLOTS AFTER IMMERSION IN FUSAYAMA SALIVA

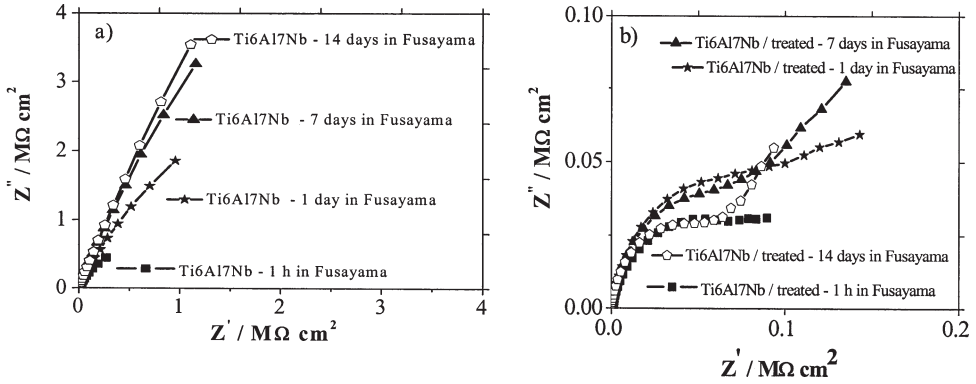

Fig. 5. Nyquist plots for untreated Ti6Al7Nb (a) and laser treated Ti6Al7Nb (b) for various immersion times in Fusayama saliva

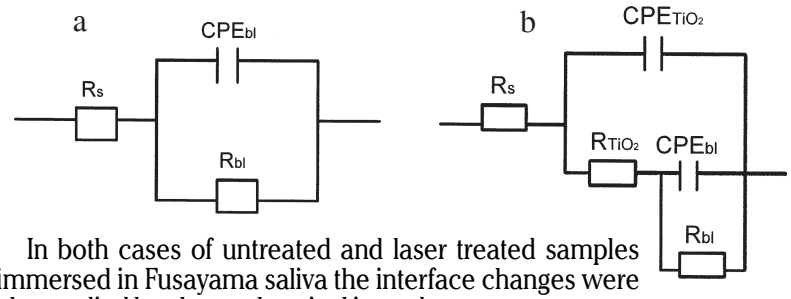

Fig. 6. Equivalent electrical circuits for untreated (a) and laser treated (b) Ti6Al7Nb

In both cases of untreated and laser treated samples immersed in Fusayama saliva the interface changes were also studied by electrochemical impedance spectroscopy, the results being given in figure 5, representing the Nyquist plots.

For untreated Ti6Al7Nb alloy (fig. 5a), an equivalent circuit with a single time constant was proposed. For the laser treated sample (fig. 5b) another circuit with two time constants was proposed: one of them corresponds to the grown oxide layer, and the second one to the barrier textured oxide layer.

Thus, the impedance data were analyzed using two equivalent circuits presented in figure 6, where R_s is the solution resistance and R_{bl} is the resistance of the native oxide barrier layer.

For the description of a frequency-independent phase shift between the applied AC potential and its current response a constant phase element (*CPE*) was used, placed in parallel with R_{bl}. The constant phase element (*CPE*) corresponds to the oxide barrier (CPE_{bl}).

In the case of treated Ti6Al7Nb alloy the equivalent circuit (fig. 6b) has two other elements, R_{TiO2} and CPE_{TiO2}, representing the resistance of the oxide grown using laser

Sample / immersion time	R_s, ($\Omega.m^2$)	CPE_{TiO2}, ($\Omega^{-1}.m^{-2}.s^n$)	n_1	R_{TiO2}, ($\Omega.m^2$)	CPE_{bl}, ($\Omega^{-1}.m^{-2}.s^n$)	n_2	R_{bl}, ($\Omega.m^2$)
Untreated Ti6Al7Nb / 1 h	$140 \cdot 10^{-4}$	-	-	-	0.16	0.78	$3.13 \cdot 10^{+2}$
Untreated Ti6Al7Nb / 1 day	$153 \cdot 10^{-4}$	-	-	-	$0.40 \cdot 10^{-1}$	0.85	$6.6 \cdot 10^{+2}$
Untreated Ti6Al7Nb / 2 days	$146 \cdot 10^{-4}$	-	-	-	$0.35 \cdot 10^{-1}$	0.86	$9.7 \cdot 10^{+2}$
Untreated Ti6Al7Nb / 7 days	$127.7 \cdot 10^{-4}$	-	-	-	$0.28 \cdot 10^{-1}$	0.87	$18.18 \cdot 10^{+2}$
Untreated Ti6Al7Nb / 14 days	$132 \cdot 10^{-4}$	-	-	-	$0.26 \cdot 10^{-1}$	0.86	$27.86 \cdot 10^{+2}$
Treated Ti6Al7Nb / 1 h	$118.5 \cdot 10^{-4}$	0.15	0.70	$1.01 \cdot 10^{+1}$	$0.40 \cdot 10^{+1}$	0.77	$1.22 \cdot 10^{+2}$
Treated Ti6Al7Nb / 1 day	$157 \cdot 10^{-4}$	$0.86 \cdot 10^{-1}$	0.79	$1.23 \cdot 10^{+1}$	$0.11 \cdot 10^{+1}$	0.78	$1.18 \cdot 10^{+1}$
Treated Ti6Al7Nb / 2 days	$143 \cdot 10^{-4}$	$0.65 \cdot 10^{-1}$	0.76	$0.23 \cdot 10^{+1}$	0.31	0.79	$0.88 \cdot 10^{+1}$
Treated Ti6Al7Nb / 7 days	$175 \cdot 10^{-4}$	$0.79 \cdot 10^{-1}$	0.82	$0.98 \cdot 10^{+1}$	0.71	0.74	$2.88 \cdot 10^{+1}$
Treated Ti6Al7Nb / 14 days	$184.5 \cdot 10^{-4}$	$0.84 \cdot 10^{-1}$	0.85	$0.69 \cdot 10^{+1}$	$0.11 \cdot 10^{+1}$	0.75	$2.92 \cdot 10^{+1}$

Table 3
ELECTRICAL PARAMETERS OF THE PROPOSED ELECTRICAL CIRCUITS FOR UNTREATED AND LASER TREATED TI6AL7Nb SAMPLES

Table 4
CORROSION RATES ESTIMATED FROM ICPMS DATA

Time, (days)	V_{corr} for untreated Ti6Al7Nb, (mm.year^{-1})	V_{corr} for treated Ti6Al7Nb, (mm.year^{-1})
0.083	$4.239 \cdot 10^{-3}$	$1.878 \cdot 10^{-2}$
1	$6.48 \cdot 10^{-4}$	$1.959 \cdot 10^{-2}$
2	$5.68 \cdot 10^{-4}$	$3.759 \cdot 10^{-2}$
7	$3.703 \cdot 10^{-4}$	$1.398 \cdot 10^{-2}$
14	$2.103 \cdot 10^{-5}$	$3.133 \cdot 10^{-3}$
37	$1.373 \cdot 10^{-5}$	$2.11 \cdot 10^{-3}$
46	$1.099 \cdot 10^{-5}$	$1.691 \cdot 10^{-3}$

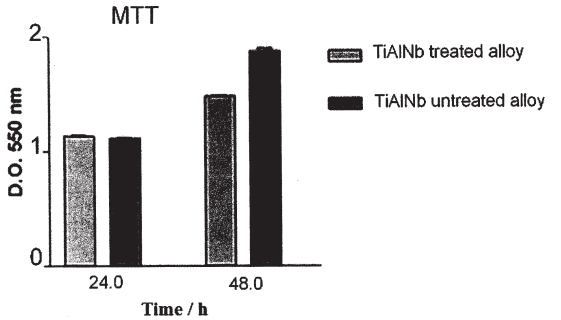

Fig. 7. Cell viability of G292 human osteoblasts on untreated and treated Ti6Al7Nb samples

treatment and the constant phase element for such an oxide.

The electrical parameters obtained after fitting the proposed circuits are presented in the table 3.

Table 3 indicated the barrier layer resistances values (R_{bl}) obtained by fitting EIS data have the same magnitude order with the polarization resistances from Tafel plots (table 2). Thus one can say that the oxide barrier layer is mainly responsible for the charge transfer resistance at the interface.

For the untreated samples, the barrier layer resistances are one magnitude order higher than the corresponding values for textured alloy, and with the increase of immersion time in saliva, R_{bl} values become higher again due to the formation on surface of a compact oxide. In time, the resistance values (R_{TiO2} and R_{bl}) increase, due to the oxide reaction with inorganic ions from Fusayama saliva (PO_4^{-3} and Ca^{+2}). The surface dissolution process and ions release (Ti, Al, Nb) in environment are blocked as a result of such complex formation on the electrode.

For the treated sample the barrier layer resistance remains almost constant during the first 24 h at $1.2 \cdot 10^{+1}$ $\Omega.m^2$, and then it decreased after 48 h at $0.9 \cdot 10^{+1}$ $\Omega..m^2$, and finally it grows in time due to surface repassivation.

Another interesting finding is that, after 14 days of immersion, R_{bl} grows nine times for the untreated sample from $3 \cdot 10^{+2}$ $\Omega..m^2$ to $27 \cdot 10^{+2}$ $\Omega.m^2$, while for the sample treated it grows only 3 times from $0.1 \cdot 10^{+1}$ $\Omega..m^2$ to $0.3 \cdot 10^{+1}$ $\Omega.m^2$. Different passivation rates and barrier layer formation may be due to the lower diffusion rate of ions through the outside oxide layer cracks at the grains boundary.

The pseudo-capacitive character of the oxide film can be observed for both treated and untreated alloys; this is corroborated with n values near 1 as well.

Corrosion rate from ion release

In table 4 the corrosion rate (V_{corr}) was estimated using the amounts of ions released in Fusayama saliva determined from ICPMS data for 46 days in the case of untreated and laser treated alloys.

The corrosion rate (V_{corr}) in mm.year^{-1} was determined using the equation:

$$V_{corr} = \frac{\text{ions.release} \cdot 365 \cdot 10}{S \cdot t \cdot d}$$ where V_{corr} = corrosion rate (mm.year^{-1}); ions release = the metallic ions release (Ti, Al, Nb) determined from ICP-MS data ($\mu g.L^{-1}$); S = surface of Ti6Al7Nb alloy immersed in Fusayama saliva solution (0.16 cm^2 for treated Ti6Al7Nb alloy and 1 cm^2 for untreated alloy); t = time (days); d = density (4.5 $g.cm^{-3}$).

The corrosion rates calculated from ICP-MS data were correlated with those obtained from Tafel plots (table 2).

For untreated sample the concentration of released ions decreases gradually during immersion due to surface passivation, but a tendency toward a constant value is observed after 14 days. This is consistent with the open circuit measurements showing that the interface changes and ion release phenomena are accompanied by potential changes in the first 14 days of immersion and reaches steady states afterwards.

In the case of laser treated Ti6Al7Nb alloy the behaviour appears to be slightly different: a competitive process, between dissolution and growth of the oxide film is taking place at the interface. The maximum of ions released is reached after a smaller period of time (48 h). A constant level is reached after 14 days of immersion and it is maintained until 46 days; the film undergoes a more important growing in thickness and acts as barrier for the release of ions.

Biocompatibility test

Figure 7 presents MTT test at 24 and 48 h using DO550 absorbance values which are proportional with the number of viable cells.

Data are presented as the average of three replicates (mean + standard deviation) (table 5) and the proliferation

Evaluation time	**Mean ± Standard deviation** (3 replicates)	
	Laser treated Ti6Al7Nb	Untreated Ti6Al7Nb
24 h	1.1256 ± 0.0110	1.1023 ± 0.0260
48 h	1.4802 ± 0.0190	1.8816 ± 0.0270

Table 5
RESULTS OF MTT FOR CELL PROLIFERATION OF G292 HUMAN OSTEOBLASTS ON UNTREATED AND LASER TREATED TI6AL7Nb SAMPLES

Comparison between P values* for	**Sampling time**	**24 h**	**48 h**
laser treated Ti6Al7Nb alloy *versus* untreated Ti6Al7Nb alloy	P (%)	> 0.05	< 0.001

Table 6
BONFERRONI'S MULTIPLE COMPARISON TEST TABLES

* P value > 0.05 no significant differences;

P value < 0.001 significant differences

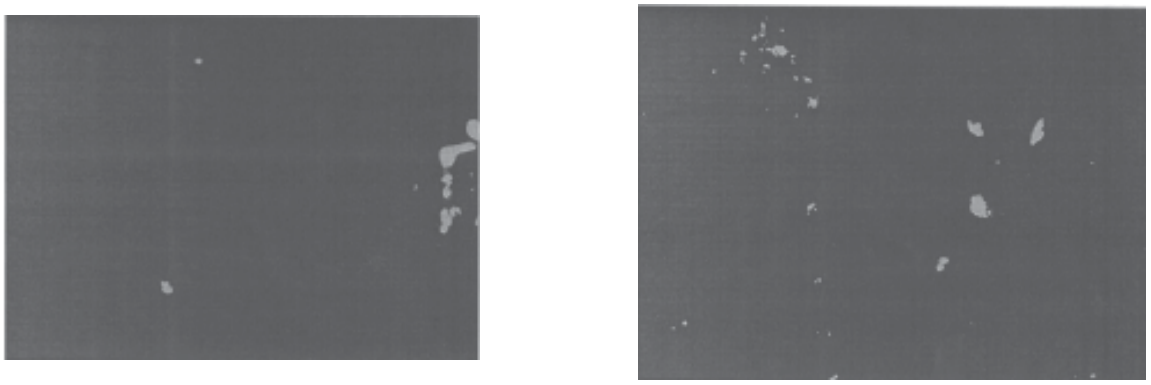

Fig. 8 Fluorescence microscopic images of G292 human osteoblasts grown on untreated (a) and laser treated (b) Ti6Al7Nb

rate (P) was measured. The difference between proliferation rates at 24 h observed for laser treated Ti6Al7Nb alloy and untreated Ti6AlNb alloy has no statistical significance. However, 48 h post seeding, the difference becomes relevant: 22 % decrease (P value < 0.001 %) (table 6). All experiments were carried out in triplicates and repeated two times.

After 24 h seeding, the number of osteoblasts is a bit higher for the treated samples, the viability being 1.1256 + 0.0110 (on untreated Ti6Al7Nb the viability is 1.1023 + 0.0260).

This fact can be explained by the fact that laser-treated surface shows grooves that may have a beneficial effect on biocompatibility and it has also a higher surface energy according to a smaller contact angle (CA), CA = 79.35°. Untreated surface is less hydrophilic, the corresponding contact angle being CA = 85.89°. The hydrophilic / hydrophobic balance is an important property in osteoblast adhesion and proliferation. The cells prefer more hydrophilic surfaces.

In the first 24 h the electrochemical stability of the oxide layer formed by laser treatment shows a better behaviour compared with untreated surface which shows continuous changes due to surface passivation, and is in agreement with the MTT values.

Roughness values are also important as well, as the cells prefer rougher surfaces, such as the treated Ti6Al7Nb alloy.

The cell viability on untreated Ti6Al7Nb alloy increases up to 1.8816 + 0.0270 after 48 h; during the same time, on laser-textured Ti6Al7Nb / oxide the cell viability is only 1.4802 + 0.0190.

This change in the cell viability after 48 h may be associated with the changes in the treated sample surface, reflected by the ion release and electrochemical measurements.

Figure 8 represents fluorescence microscopic images for both alloys after 48 h. Cell attachment on the analyzed surfaces was assessed by visualization in fluorescence microscopy of the adhered cells labelled with FITC-phalloidin for actin localization. Adhesive cell interactions mediated by extracellular matrix (ECM) were evaluated by fluorescent immunocytochemical analysis of fibronectin secretion.

The images in figure 8 indicate a good adhesion and similar aspects for treated and untreated alloys. Samples textured for longer time do not have a better behaviour from the point of view of corrosion and cell viability; however, according to literature [25] and our data, the existence of cracks may be used for the enhancement of bone - implant strength.

Conclusions

The surface characterization of laser-treated Ti6Al7Nb alloy shows cracks and grooves in SEM and AFM analysis and small shifts to more hydrophilic values in contact angle data.

Such cracks and grooves may improve bone implants strength, despite the fact that cracks are related, as expected, with an increase in corrosion rate.

The untreated Ti6Al7Nb surface has a better behaviour to corrosion compared to treated alloy taking into account the smaller corrosion rates, even if the corrosion potentials for treated samples are shifted in anodic direction at all times. These changes are supported by electrochemical (EIS and Tafel plots results) and by ion release data.

Despite the fact that the corrosion rate is increased after laser treatment, cracks and grooves may improve bone implants strengths and cell adherence.

However, the effect of working conditions is related to the rate of cell viability.

Acknowledgements. The authors gratefully acknowledge financial support from the Romanian National CNCSIS, Grant IDEI PCCE code 248.

References

1.BALAZIC M., KOPAC J., JACKSON M.J., AHMED W., Int. J. of Nano and Biomaterials., **1**, 2007, p. 3.
2.CORBAN M., ROMAN I., TRUSCA R., DINISCHIOTU A., CARCEANU I., STAN N., FRATILA C., Rev. Chim.(Bucharest), **63**, nr. 1, 2012, p. 22.
3.KOBAYASHI E., WANG T.J., DOI H., YONEYAMA T., HAMANAKA H., J. Mater. Sci. Mater. Med,. **9,** 1998, p. 567.
4.POPA M.V., DEMETRESCU I., IORDACHESCU D., CIMPEAN A., VASILESCU E., DROB P., VASILESCU C., ISTRATESCU M., Mater. Corros., **58,** 2007, p. 667.
5.VARÍOLA F., VETRONE F., RICHERT L., JEDRZEJOWSKI P., YI J.H., ZALZAL S., CLAIR S., SARKISSIAN A., PEREPICHKA D.F., WUEST J.D., ROSEI F., NANCI A., Small, **5**, 2009, p. 996.
6.SHUKLA A.K., BALASUBRAMANIAN R., Corros. Sci., **48**, 2006, p. 1696.
7.CHRISEY D.B., HUBLER G.K., Pulsed laser deposition of thin films, J. Wiley, New York, America, 1994, p. 648.
8.KURELLA A., DAHOTRE N.B., J. Biomater. Appl.**, 20,** 2005, p. 5.
9.LIU X., ZHAO X., DING C., CHU P.K., Surf. Coat. Technol.**, 201,** 2007, p. 6878.
10.MANOLE C.C., PIRVU C., DEMETRESCU I., Key Eng. Mater., **415,** 2009, p. 5.
11.MÎNDROIU M., PIRVU C., ION R., DEMETRESCU I., Electrochim.Acta., **56**, 2010, p. 19.
12.IONITA D., MAZARE A., PORTAN D., DEMETRESCU I., Met. Mater. Int., **17**, 2011, p. 321.
13.BRAGA F.J.C., MARQUES R.F.C., FILHO E.D.A., GUASTALD A.C., Appl. Surf. Sci.**, 253,** 2007, p. 9203.

14.PFLEGING W., BRUNS M., WELLE A., WILSON S., Appl. Surf. Sci.**, 253,** 2007, p. 9177.
15.SOCOL G., TORRICELLI P., BRACCI B., ILIESCU M., MIROIU F., BIGI A., WERCKMANN J., MIHAILESCU I.N., Biomater., **25,** 2004, p. 2539.
16.KRSTULOVIĆ N., MILOŠEVIĆ S., Appl. Surf. Sci.**, 256,** 2010, p. 4142.
17.POPA M.V., DROB P., RĂDUCANU D., CASTRO J.R., MIRZA ROSCA J.C., Rev. Chim.(Bucharest), **58**, no. 2, 2007, p. 179.
18.MÎNDROIU M., CICEK E., MICULESCU F., DEMETRESCU I., Rev. Chim., **58**, 2007, p. 898.
19.VITTE J., BENOLIEL A.M., PIERRES A., BONGRAND P., Eur. Cell Mat., **7**, 2004, p. 52.
20.CIMPEAN A., POPESCU S., CIOFRANGEANU C.M., GLEIZES A.N., Mater. Chem. Phys., **125** , 2011, p. 485.
21.TIAN Y.S., CHEN C.Z., LI S.T., HUO Q.H., Appl. Surf. Sci., **242**, 2005, p. 177.
22.HE R.J., WANG H.M., Mater. Sci. Eng., **A 527**, 2010, p. 1933.
23.SIMA C., GRIGORIU C., Thin Solid Films, **518**, 2009, p. 1314
24.BANDYOPADHYAY A., ESPANA F., BALLA V.K., BOSE S., OHGAMI Y., DAVIES N.M., Acta Biomater., **6**, 2010, p. 1640.
25.ZIELI SKI A., DZIADO A., SERBI SKI W., JA D EWSKA M., Adv. Mater. Sci., **8**, 2008, p. 94.
26.MÎNDROIU V.M., PÎRVU C., POPESCU S., DEMETRESCU I., Rev. Chim.(Bucharest), **61**, no. 4, 2010, p. 390.
27.BERRIDGE M.V., TAN A.S., MCCOY K.D., WANG R., Biochemica, **4**, 1996, p. 14
28.MOSMANN T., J. Immunol. Methods., **65**, 1983, p. 55.
29.MINDROIU V.M., CICEK E., CIUBAR R., Mol. Cryst. Liq. Cryst., **486**, 2008, p. 120.
30.MILOSEV I., KOSEC T., STREHBLOW H.H., Electrochim. Acta, **53**, 2008, p. 3547

Manuscript received: 22.07.2013